Research Paper

Normalization of time series DMSP-OLS nighttime light images for urban growth analysis with Pseudo Invariant Features

Ye Wei [a], Hongxing Liu [b], Wei Song [c], Bailang Yu [d], Chunliang Xiu [a],[*]

[a] School of Geographical Science, Northeast Normal University, Changchun, Jilin 130024, China
[b] Department of Geography, University of Cincinnati, Cincinnati, OH 45221, USA
[c] Department of Geography and Geosciences, University of Louisville, Louisville, KY 40292, USA
[d] Key Laboratory of Geographic Information Science, Ministry of Education, East China Normal University, Shanghai 200241, China

HIGHLIGHTS

- A technique for normalizing time series DMSP-OLS nighttime light data is proposed.
- Concept of desaturated Pseudo Invariant Features is proposed.
- Dividing time series into sub time series benefits to improve accuracy.
- The spatio-temporal evolution of Central Liaoning region in China is investigated.

ARTICLE INFO

ABSTRACT

Previous studies demonstrated that DMSP-OLS stable nighttime light data are useful data source for delineating urban areas. However, the nighttime light data acquired in different years are not directly comparable, due to the variations in atmospheric condition from year to year and the periodic change in satellite sensor. This makes it difficult to use the time series nighttime light data for urban growth analysis. This paper presents a novel technique for normalizing time series DMSP/OLS nighttime light data and deriving urban detection threshold using Pseudo Invariant Features (PIFs). Our technique consists of three steps: (1) estimate an optimal threshold value for urban area detection for a reference year, when high resolution image data are available for some local areas. (2) Based on the irreversible nature of urbanization process, determine a set of PIFs, which are deemed as urban areas and did not exhibit significant change in nighttime light condition during the study period. (3) Normalize the time series DMSP-OLS data sets based on the PIFs and linear regression, determine optimal threshold values for urban area detection for all years based on the reference year threshold value, and extract urban areas accordingly. This technique was successfully applied to time series DMSP-OLS nighttime light images of the Central Liaoning region in China. Patterns of this urban agglomeration's spatial–temporal evolution from 2000 to 2010 were mapped and analyzed. The reliability and spatial accuracy of this technique were evaluated with multitemporal Landsat TM images. The technique was proved accurate and effective.

© 2014 Elsevier B.V. All rights reserved.

1. Introduction

The U.S. Defense Meteorological Satellite Program Operational Linescan System (DMSP-OLS) has a unique capability in detecting and recording lights present at night on the Earth's surface (Croft, 1978). The OLS sensors record broadband emissions (lights) in visible near-infrared (VNIR) portion (0.5–0.9 μm) of the spectrum (Elvidge et al., 1997). As the OLS sensors use a photo multiplier tube (PMT) at least four orders of magnitude more sensitive than those used in any other satellite systems, they can sense even faint sources of nighttime lights (Elvidge, Baugh, Kihn, Kroehl, & Davis, 1997). Since 1992, nine DMSP satellites (F10, F11, F12, F13, F14, F15, F16, F17, F18) have been launched with OLS sensors onboard, and four of them (F15, F16, F17, and F18) are still operational at present. DMSP satellites are in a sun-synchronous near-polar orbit at an altitude of 830 km above the surface of the earth, and the nighttime light image swath of the DMSP-OLS sensor covers 3000 km

* Corresponding author at: School of Geographical Science, Northeast Normal University, 5268 Renmin Street, Changchun, Jilin 130024, China. Tel.: +86 13353296232.
E-mail addresses: weiy742@nenu.edu.cn (Y. Wei), hongxing.liu@uc.edu (H. Liu), wei.song@louisville.edu (W. Song), blyu@geo.ecnu.edu.cn (B. Yu), xiucl@nenu.edu.cn (C. Xiu).

wide ground surface. The combination of day/night and dawn/dusk DMSP satellites provides global coverage twice per day (Elvidge, Erwin, et al., 2009).

Nighttime lights detected by DMSP-OLS sensors are generated by a variety of sources, including human settlements, clouds illuminated by moonlight, forest fires, fishing boasts, and gas flares (Elvidge et al., 1999). The lights from human settlements, particularly urban areas, represent the primary contributing component, which is distinguished from other source components by its temporally stable and persistent nature. Stable light image products have been produced to map urban areas by eliminating and reducing the effects of cloud, ephemeral lights and other environmental factors on the raw nighttime light intensity recorded by DMSP-OLS sensors. Since the outdoor lighting is widely used by human society, nighttime lights can reflect the presence of land development or human activities (Elvidge, Erwin, et al., 2009). Urban areas in modern societies, in particular, are brightly lighted at night. Previous studies have demonstrated that the stark contrast between lighted urban areas and unlighted rural areas makes it much easier to delineate and distinguish urban areas from surrounding rural areas on the DMSP nighttime light images (Henderson, Yeh, Gong, Elvidge, & Baugh, 2003).

Imhoff, Lawrence, Stutzer, and Elvidge (1997) mapped the urban areas for the continental United States by using a thresholding technique based on the nighttime light data. In their study, thresholds were first determined for Chicago, Sacramento and Miami metropolitan areas respectively by using a perimeter mutation detection approach. The average value of thresholds for the 3 metropolitan areas was then used to detect urban areas from nighttime light imagery for the entire US. However, the mutation detection approach is difficult to implement in practice, and a single threshold value may not be appropriate and suitable for the entire country. Sutton, Roberts, Elvidge, and Baugh (2001) recognized the limitations of using a single threshold for a global analysis of nighttime light image data. They used 40%, 80% and 90% of a threshold value for different regions in the world to detect and calculate lighted area and aggregate population. However, choosing between 40%, 80% and 90% of the threshold is kind of arbitrary and not scientifically justified. A similar approach with varying threshold values was employed by a number of other studies (Milesi, Elvidge, Nemani, & Running, 2002; Sutton, Cova, & Elvidge, 2006; Sutton, 2003). Henderson et al. (2003) used DMSP stable and radiance-calibrated light image to delineate urban boundaries, while Landsat TM imagery was used as auxiliary information to determine the optimal threshold. Instead of Landsat TM image, He et al. (2006) used the census data as ancillary information to determine the threshold, but the accuracy of the resulting threshold is questionable due to the poor quality and inconsistency of the census data. Zhang and Seto (2011) demonstrated the utility of multi-temporal nighttime light data to proxy urbanization dynamics by establishing significant positive linear relationship between urbanization dynamics derived from DMSP-OLS nighttime light images and other independent data sources including U.S. National Land Cover Database (NLCD) and World Bank urban population growth data. An iterative unsupervised classification method was applied to 1992–2008 multi-temporal nighttime light data and urbanization dynamics in India, China, Japan, and the United States were mapped. This study further illustrated that oversaturation of nighttime light data and differences in the radiometric signatures across DMSP-OLS satellites could blur the temporal and spatial signature of urban change and make analytical results biased, thus calling for more accurate calibration of multi-temporal nighttime light data. Previous studies also show that the stable light image products have a tendency to overestimate the extent of urban area, which is referred to as "blooming" or "overglow" phenomenon. The blooming phenomenon is due to the combination of a number of factors:

coarse spatial resolution, the accumulation of geolocation errors in the image compositing process (Small, Pozzi, & Elvidge, 2005), atmospheric scattering effect (Doll, 2008) and water surface reflection effect.

Henderson et al. (2003) showed that no single threshold is suitable for detecting urbanized areas from DMSP nighttime light data for different metropolitan regions. They also pointed out that DMSP light data collected in different years are not directly comparable, due to the variations in gain settings, sensor degradation, and the change in atmospheric condition. To perform time series analysis of DMSP nighttime light data for urban growth detection, a threshold value has to be determined separately for each year. Some studies addressed the inter-annual comparability issue of temporal DMSP nighttime light images. Elvidge, Ziskin, et al. (2009) assumed that there was little change in the nighttime light intensity of Sicily, Italy and used it to fit a second order regression model to perform an intercalibration between other annual light composites and 1999 light image composite from satellite F12 for the entire world. The use of a single site for nighttime image calibration may remove the global bias caused by the change in satellite sensors and sensor gain setting. But the local and regional biases caused by the spatio-temporal changes in atmospheric condition, such as weather or climate factors which can affect the atmospheric transmission of nighttime light, cannot be removed. Witmer and O'Loughlin (2011) identified some "stable" cities and towns and then attempted to remove inter-annual systematic differences between nighttime light image composites based on the statistical distribution of pixel digital number (DN) values of the "stable" cities and towns. Liu, He, Zhang, Huang, and Yang (2012) proposed a method for systematically correcting multi-year and multi-satellite nighttime stable light (NSL) data. They used a second-order regression model to calibrate DN values for different satellites to improve nighttime light data comparability over the study period, using City of Jixi as the calibration area and 2007 nighttime light data from satellite F16 as the reference dataset. They performed an intra-annual data composition using averaged DN values of two NSL images and removed intra-annual unstable lit pixels. They further removed inconsistencies in the multi-year dataset and corrected DN values for consistently lit pixels based on the assumption that the DN value of a lit pixel in an early image would not exceed its DN value in a later image. With the help of ancillary land use/cover data, optimal thresholds in urban area detection in the time series were determined for different economic regions in China. Although these heuristic methods may be able to remove "regional radiometric" biases and help improve the continuity and comparability of multi-temporal DMSP-OLS data, they also pose serious challenges in the application. It is not always easy to identify the stable reference city or town in practice. Also, these methods require ancillary information, such as high resolution images or census data, for data calibration and the determination of urban detection threshold value for DMSP nighttime light image each year. In reality, the required ancillary information is rarely available at desired spatial scales and for all years, particularly for a long-term time series. The lack of sufficient ancillary reference data often prevents the use of time series DMSP nighttime light data for urban growth analysis.

Other attempts have been made to normalize the optical satellite images acquired in different seasons and in different years (Canty & Nielsen, 2008; Hadjimitsis, Clayton, & Retalis, 2009; Schott, Salvaggio, & Volchok, 1988). Schott et al. (1988) used the Pseudo Invariant Features (PIFs) to normalize the multiple temporal Landsat TM images for the same area, in which the PIFs were man-made objects whose reflectivity is nearly constant, independent of the imaging conditions and seasonal or biological cycles. Based on these PIFs, linear transform and the histogram-matching technique were used to quantitatively transform multiple temporal Landsat TM images with reference to one specified image.

The PIFs based method has also been used by Clark, Suomalainen, and Pellikka (2011) to normalize multi-temporal SPOT images and by Philpot and Ansty (2011) to normalize hyperspectral images acquired at different times. For natural scenes, deep water bodies, beach sands and other natural features are often selected as PIFs, since their spectral reflectivity virtually keeps the same, without too much seasonal and phonological variation. However, none of previous studies used the concept of PIFs to normalize DMSP-OLS images acquired in different years. Reliable urban change analysis by fully exploiting time series DSMP-OLS light images calls for an effective and practical method for DSMP-OLS image normalization.

This study represents the first attempt to utilize the concept of Pseudo Invariant Features (PIFs) directly in the determination of urban detection threshold values for entire time series of DMSP-OLS nighttime light images. In this study, we present a novel, PIF-based technique for normalizing time series DMSP-OLS nighttime light images and determining urban detection threshold values. With this technique, we are able to determine the optimal urban area detection thresholds for all years, using ancillary reference data only for the reference (base) year or just a few years of the time series. Our technique has largely relaxed the demand for the ancillary reference data and made the time series analysis of DMSP nighttime light data possible with only limited ancillary data.

In the following sections, we will first introduce the data sets used in our analysis, and then describe our new method in detail. Next, a case study is presented to illustrate and evaluate our new method. Finally, we summarize our main findings and outline the directions for future research.

2. Data sets

2.1. DMSP-OLS stable light data

The National Oceanic and Atmospheric Administration (NOAA) National Geophysical Data Center (NGDC (2011)) has processed the archived DMSP-OLS data into different types of nighttime light image products. The recently published Version 4 DMSP-OLS data products include three types of image composites spanning from 1992 to 2010: cloud-free coverage composite, average visible composite, stable lights composite. These image composites were created by using cloud-free observations of all the available archived DMSP-OLS smooth resolution data for each calendar year. For some years, two DMSP satellites were operating and collected two sets of nighttime light data. In that case, image composites were produced from observations of each satellite. Observations contaminated by solar glare, moonlight, and the aurora borealis in the northern hemisphere have been excluded in the creation of these annual composite products. The grid cell size of these image composites is 30 arc second (approximately 1 km), oversampled from the original DMSP-OLS smooth mode observations at a spatial resolution of 2.7 km (Small, Elvidge, Balk, & Montgomery, 2011). The pixel value of the cloud-free coverage composite represents the total number of cloud-free observations that were recorded for the pixel during the calendar year. The average visible composite contains the average value of light intensity of all cloud-free observations for every pixel during the calendar year, and it includes the effect of ephemeral events like wild fires. The stable lights image composite was created by further cleaning up the ephemeral light sources such as wild fires, lightning and fishing boats. The pixel value of the stable light image composite represent the average of all light intensity values observed in cloud-free days in a calendar year from temporally stable sources such as cities, towns, villages, industrial sites, and persistent gas flares. The pixel value has 6-bit radiometric quantification levels, ranging from 0 to 63 (Doll, 2008). Areas without cloud-free observations in a calendar year are

indicated by the value of 255. Stable light images may suffer from the saturation problem, which is often associated with urban centers where nighttime lights are so strong that their light intensities exceed the maximum radiometric quantification level (63) of the OLS sensors and their DNs are simply truncated to the highest possible value of 63. The radiance calibrated DMSP-OLS light images created from DMSP-OLS low-gain mode observations overcome the saturation problem (Elvidge et al., 1999). However, such radiance calibrated nighttime light images exist only for a few specific years. At present, the time-series stable light images represent the best available data products for studying temporal evolution of urban settlements and thus were used in this study.

2.2. Landsat TM images

In this study, Landsat TM images were used as ancillary information to help determine the threshold value for segmenting the DMSP-OLS image into urban and non-urban regions for the reference year. Landsat TM imagery has six optical spectral bands with a 30 m spatial resolution. Impervious surface can be delineated as urban areas from the Landsat TM imagery through visual interpretation or automated classification approach. Due to its relatively fine spatial resolution, urban areas derived from Landsat TM imagery can be treated as ground truth in determining the threshold value for the DMSP-OLS nighttime light image, which has much coarse spatial resolution (2.7 km). As demonstrated in Elvidge et al. (2004), we manually delineated urban areas as a set of polygons through on-screen visual interpretation of Landsat TM images in ArcGIS environment. The Landsat images were also used to validate urban detection results from DMSP-OLS nighttime light images for several selected years. The DMSP-OLS nighttime light images and Landsat TM images were georeferenced using ALBERS equal-area conic projection with the central meridian of 122° W and two standard parallels of 43° N and 44° N. The geolocation accuracy of the DMSP-OLS images is relatively poor. We observed a systematic geolocation shift of about 1–2.5 pixels toward north or northwest direction relative to the Landsat TM image, a phenomena once revealed by Henderson et al. (2003). In their work, a shift of 1.7–2.8 pixels toward northeast was observed in Beijing. We performed the co-registration with reference to Landsat TM images to correct the geolocation bias of DMSP images.

3. Methods

The DMSP-OLS satellite sensors record the nighttime light energy emitted from the Earth's surface. Due to the concentration of human activities, settlements and facilities, urban areas emit much stronger and more intensive lights during nighttime than the surrounding rural areas. Overall, the urban land use change is an irreversible process. Once an area is changed from rural to urban land use, it normally would remain urban (Zhang & Seto, 2011). For many well-established and mature urban neighborhoods, the intensity of night light emitted from them would keep virtually constant. Such urban neighborhoods are denoted as Pseudo Invariant Features (PIFs) in the sense that the nighttime light intensity of these urban features would not vary too much in time. The concept and method of invariant areas and stable pixels in time series of images have been demonstrated in previous research (Coppin & Bauer, 1994; Hall, Strebel, Nickeson, & Goetz, 1991; Lenney, Woodcock, Collins, & Hamdi, 1996). In this study, we use these PIFs in different years of DMSP-OLS images to capture the type of transformation relationship to help normalize time series data and determine different urban detection threshold values. For PIFs, the difference in the recorded nighttime light intensity between different years can be attributed to the variation of atmospheric

conditions (e.g. weather or climate factors) and changes in DMSP-OLS sensor and sensor gain setting. Therefore, we are able to use the PIFs to compute the correction term denoting the effects caused by changes in the atmospheric condition and DMSP-OLS sensors. By applying the computed correction term, we can normalize the DMSP-OLS image data between different years and make them comparable in time.

For a relatively small region, we can safely assume that atmospheric condition at different locations within the region is similar in a calendar year. Under this assumption, we can use a single threshold for the entire region to detect urban areas for a specific year. However, due to the variation of atmospheric condition from year to year and the changes in DMSP-OLS sensor as well as sensor gain setting, the DN values of DMSP-OLS nighttime light image data from different years are not comparable. Therefore, the threshold value determined for one year cannot be directly extended to other years for urban area detection.

The fundamental idea of our method is to use PIFs to normalize time series DMSP-OLS images and to make them comparable between different years. After the normalization, we can determine optimal threshold value for each year of the entire time series of DMSP-OLS nighttime light data based on only limited amount of available ancillary information.

Our technique consists of three steps: (1) estimate the threshold value for urban area detection for a reference year, in which high resolution image data like Landsat TM are available for some local areas. (2) Based on the irreversible nature of urbanization process, determine a set of PIFs, which are deemed as urbanized areas where there is not much change in nighttime light intensity during the period of the study. (3) Normalize the time series DMSP-OLS data sets based on the PIFs, determine optimal urban detection threshold values for all years based on the reference year's threshold, and then extract urban areas accordingly.

3.1. Estimate the urban detection threshold value for the reference year

The key to accurately delineate the urban boundaries is to identify a suitable threshold value for segmenting a DMSP-OLS image. On DMSP-OLS nighttime light images, urban areas have a large DN value in general and are shown as brightly lit patches. To numerically delineate the boundaries of urban areas, we need to find a suitable threshold value to segment the pixels of a DMSP nighttime light image into two categories: those with a DN value equal to or larger than the threshold indicating urban areas, and those with a DN value less than the threshold indicating rural areas. In this study, the threshold value for the reference year was calibrated and determined by using Landsat TM imagery.

An iterative searching method, similar to that used by Henderson et al. (2003) and Liu et al. (2012), was employed to determine the optimal reference year urban detection threshold. First, we manually delineated urban areas on-screen as a set of polygons in ArcGIS environment by visually interpreting Landsat TM images for the entire study area, and calculated the total area of these urban polygons. Next, a series of incremental threshold values starting at 1 was used to segment the DMSP nighttime light image into a binary image, consisting of two different types of pixels: urban pixels and rural pixels. The total area and overall shape of urban pixels extracted from DMSP image at each iteration were then compared with the urban land use areas extracted from Landsat TM image. We determined the optimal urban detection threshold for the DMSP image such that the extracted lit urban area at that threshold value most closely matched the urban polygons derived from the ancillary Landsat TM image in both total area and spatial extent.

3.2. Determine desaturated Pseudo-Invariant Features (PIFs)

Due to the dissimilarity in the image formation between the DMSP nighttime light images and multispectral optical images like Landsat TM and SPOT images, the PIFs have to be defined and identified for DMSP-OLS nighttime light images in a different manner. Instead of using the terrain features with constant spectral reflectivity as PIFs to normalize multi-temporal optical satellite images, the features that emit temporally stable and invariant nighttime lights should be used as PIFs for the DMSP-OLS image normalization. The fully developed and stable urban districts, where no significant further development and changes occur, satisfy the stable nighttime light requirement and can be used as PIFs. In addition, the DMSP-OLS images have a much coarser spatial resolution but cover much larger ground in comparison with the moderate resolution optical satellite images. Therefore, PIFs are required for normalizing multi-temporal DMSP-OLS images.

There are several urban form models in literature describing urban morphology, land use, the spatial distribution of people, buildings, and human activities across a city's landscape. Those include concentric zone model (Burgess, 1925), sector model (Hoyt, 1939), multiple nuclei model (Harris & Ullman, 1945), and more complex models (Shevsky & Bell, 1955; Mann, 1965; Murdie, 1969). For each individual urban patch (district), it appears that the Ernest Burgess's concentric zone model captures most of the urban spatial pattern observed on DMSP-OLS light images. The concentric zone model conceptualizes urban land use in concentric rings radiated from the central business district (CBD) or downtown in the middle of the urban area. According to Burgess, urban growth is a process of expansion and reconversion of land uses, with a tendency of each inner zone to expand into the outer zone. As the city grew and developed over time, the expansion of the CBD/downtown would invade residential neighborhoods immediately surrounding it and cause them to expand outward. The process continued with each successive neighborhood moving further from the urban center. This successive expansion process forms orderly spatial arrangement of a set of concentric rings with different land use types around the urban center, in which the concept of distance decay is embedded. Population density and land use intensity decrease with increasing distance from urban center in general. Suburbanization and the conversion of once-agricultural or other natural resource lands into urban land uses often happen in more economically developed countries. But in recent years, similar process, which has led to low-density residential and commercial development at the urban fringe, is becoming increasingly apparent in newly industrialized countries such as China (Theobald, 2001). Various remote sensing studies proved that urban forms in most of Chinese cities closely resembled the concentric ring pattern (Liu, Zhan, & Deng, 2005; Seto & Fragkias, 2005; Zhang, Wu, Zhen, & Shu, 2004). We observed that the nighttime light intensity or the DN values of most urban patches show a concentric zone pattern, when it is represented as a set of light intensity contour lines. The light intensity cross-section profile peaks at the urban center, gradually decreases from urban center to urban peripheral, and levels out at the urban-rural boundary. For a relatively large urban center, the light intensity forms a high plateau in the center due to the saturation, surrounded by successive concentric urban zones with decreasing light intensity. This apparent concentric zone pattern of nighttime light intensity closely, although not perfectly, corresponds to urban development patterns, reflected by population density, building density, intensity of urban activities and infrastructure, etc.

Based on the high resolution Landsat TM image data, we delineated urban areas as polygon features for the base year of the time series. Owing to the irreversible nature of the urbanization process, these polygon features delineated for the base year would
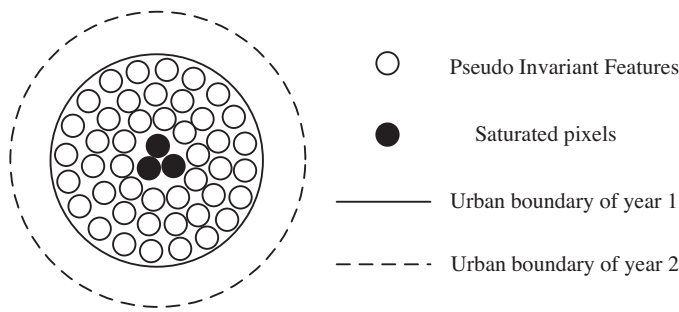
Fig. 1. Schematic diagram of desaturated PIFs.

remain urban in subsequent years. For each urban polygon delineated, DMSP-OLS pixels falling inside were examined. Pixels with a DN value larger than 62 were eliminated as they are considered to be saturated. As discussed above, the saturated areas often form high plateaus in the nighttime light images, corresponding to the CBDs or highly developed urban industrial districts in the urban areas (Elvidge et al., 1999). By eliminating possibly saturated pixels inside each urban polygon, we created donut shape polygon features. Inside the donut polygons, there is apparent spatial variation in the nighttime light intensity with changing distance to the urban center. However, the nighttime light intensity inside these donut polygons is considered to be temporally stable and invariant. Therefore, these donut polygons were used as pseudo-invariant features in this study and labeled as desaturated PIFs (see Fig. 1).

3.3. Normalization methods and urban area extraction

The light intensity of pixels within desaturated PIFs varies from the urban center to urban fringes. We used a linear regression model to relate light intensity values of pixels within desaturated PIFs between the reference year (base year 0) and a subsequent year t as below:

$$DN_t = \alpha + \beta \times DN_0 \tag{1}$$

where DN_0 is the light intensity for the reference year (base year 0), and DN_t is the light intensity for year t for the same pixel, α and β are intercept and slope of the linear regression model. Through this linear regression model, the DMSP nighttime light image for year t can be normalized with reference to the base year 0.

Given the urban detection threshold value T_0 derived for the reference year (base year 0) using Landsat TM image, the urban detection threshold value for year t, T_t, can be determined by the following equation:

$$T_t = [\alpha + \beta \times T_0] \tag{2}$$

For the robustness of the linear regression method, outliers were eliminated before we calibrated the final regression model. Specifically, we first ran the regression model from the whole raw data to obtain the predictive DN values, and then computed the residuals δ between the predictive and observed DN values. In general, δ should obey normal distribution $N(0, \sigma^2)$. Based on δ, the standardized residual δ^* was then computed by the following equation:

$$\delta^* = \frac{\delta - \bar{\delta}}{\sigma(\delta)} \tag{3}$$

where $\bar{\delta}$ is the average of δ, and $\sigma(\delta)$ is the standard deviation of δ. Standardized residuals δ^* should obey normal distribution $N(0, 1)$, with a probability of 0.05 for δ^* falling outside interval $(-2, 2)$. Using this criterion, if the standardized residuals δ^* of falling sample point falls outside interval $(-2, 2)$, the sample point was eliminated as outlier at the 95% confidence level.

After the urban detection threshold was determined for each year, we extracted urban areas from DMSP images accordingly. As used by some previous studies (He et al., 2006; Liu, He, Zhang, Huang, & Yang, 2012), we assumed that urban pixels extracted in the previous year nighttime light image would not disappear in subsequent years in the process of urban area extraction. They would remain as urban areas due to the irreversible nature of urbanization. In this way, we ensured that urban areas detected would be consistent in the time series and follow a spatial pattern of continuous outward growth.

4. A case study

4.1. The case study area

Our study area is the central region of Liaoning province in China (Fig. 2).It covers a geographical area of about 15,360 km^2 between 40°57′ N and 42°8′ N in latitude and 122°47′ E to 124°10′ E in longitude. The region is highly urbanized, and the Central Liaoning urban agglomeration is located in this region. The region has long been the largest heavy industrial base in China, known as eastern "Ruhr" in China. At present, heavy industry is still an important sector for the regional economy. In the 1990s, the economy and urbanization in this region developed at a quite slower pace, in comparison with the eastern coastal area of China which experienced an economic boom due to economic reform and open-door policies. However, with the implementation of the northeast old industrial base revitalization program, the economic development and urbanization of the region have regained momentum and speeded up since 2003 (Zhang, 2008).

There are five big cities in this region, including Shenyang, Fushun, Anshan, Benxi and Liaoyang (see Fig. 2). According to the sixth population census of China, the populations of these cities in 2010 are 8.1 million, 2.13 million, 3.64 million, 1.71 million and 1.86 million, respectively. These cities share a common characteristic in that heavy industry sector plays the most important role in their economy. For example, Shenyang was famous for its equipment manufacturing; Fushun and Liaoyang were well known for their petrochemical industry; Anshan and Benxi were the most important bases in China's steel industry. For a long time, these heavy industries had dominated the economy of these cities. However, new changes are emerging across the region, with the support of the northeast old industrial base revitalization program. All of cities are experiencing a radical overhaul of local economy from being strongly dominated by heavy industries to a more diversified and consumer-oriented structure. Shenyang has been quite successful in the economic transformation, becoming a political, economic, financial and cultural center of Northeast China. Other cities also have made significant progress in economic restructuring. For instance, pharmaceutical industry has become a new pillar in Benxi's urban economy. As a result of this drastic process of economic development and restructuring, noticeable spatial and temporal dynamics of the Central Liaoning urban agglomeration would be expected.

We obtained and processed annual DSMP-OLS stable nighttime light image data for the period between 2000 and 2010. The year 2000 was used as the reference year (base year 0), and Landsat TM image is available for this year. The optimal threshold value for the reference year 2000 was determined by using Landsat imagery and the iterative searching method. Urban detection threshold values for the subsequent ten years from 2001 to 2010 were determined based on desaturated PIFs and linear regression method. In addition, Landsat TM images for 2002, 2006, 2009, and 2010 were also obtained and processed. They helped validate and evaluate the
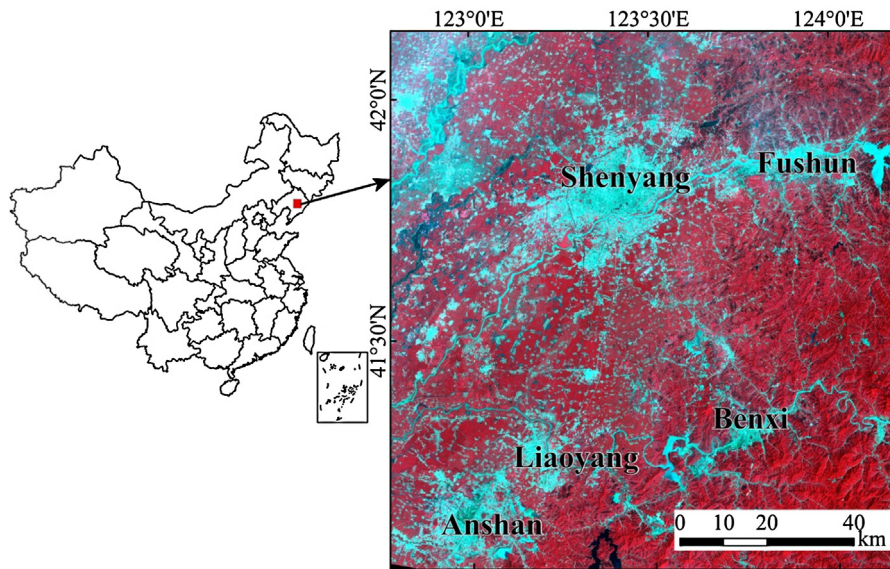
Fig. 2. Location map and 2010 Landsat TM image (bands 4, 3, 2) of Central Liaoning urban agglomeration.

4.2. Results

We first visually interpreted 2000 Landsat TM multispectral image and manually delineated urban areas on computer screen as a set of vector polygons. The iterative searching method was then applied to the 2000 DMSP-OLS stable light image "F142000" to derive the optimal urban detection threshold for 2000. The optimal threshold value (T_{2000}) for the reference year 2000 is 40. After urban areas were extracted from 2000 DMSP-OLS image, saturation patches were delineated in ArcGIS by identifying pixels with DN value larger than 62. By removing saturation patches, we created the desaturated PIFs (Fig. 3). The linear regression method was then applied to desaturated PIFs to determine the optimal urban detection threshold value for each of the subsequent years.

By using the linear regression method with desaturated PIFs, we estimated the regression coefficients α and β in Eq. (1) for the years from 2001 to 2010. Given the threshold value $T_{2000} = 40$ for the reference year (2000), the urban detection threshold values for DMSP-OLS nighttime light images acquired during 2001–2010 were estimated using Eq. (2). The linear relationship is quite obvious for most years, but it appears to be deviated from linear by many nearly saturated pixels in some years. The DN value of a lit pixel in a stable DMSP image represents the average of cloud-free observations observed in a calendar years. Although the DN values of nearly saturated pixels in a stable DMSP light image are less than 63, some of cloud-free daily observations in the calendar year may in fact be saturated with a DN value of 63. Therefore, the nearly saturated pixels are not reliable for regression analysis. To ensure the reliability of the regression method, we removed not only saturated pixels but also nearly saturated pixels (DN > 59) for both the reference year and each of the subsequent years in creating desaturated PIFs. When two light images acquired by different DMSP-OLS satellites for the same year are available, a threshold value was separately calculated for each individual DSMP-OLS image for that year. For instance, threshold values were calculated for two stable nighttime light images "F152006" and "F162006" for 2006, which were produced from observations of Satellite F15 and Satellite F16 in 2006. Table 1 shows the results of the linear regression method based on desaturated PIFs.

4.3. Validation and accuracy assessment

To validate our desaturated PIF-based linear regression method, we obtained and processed Landsat TM images for 2002, 2006, 2009, and 2010. Using the same image interpretation procedure as for the reference year, we manually delineated urban patches as vector polygons for these four years, which were treated as ground truth. By overlaying the urban polygons interpreted from Landsat images with those from DMSP-OLS light images of the same years, we determined optimal urban detection threshold values for DMSP-OLS light images for these four years. By comparing the threshold values and urban areas detected using our desaturated PIF-based linear regression method with the optimal threshold
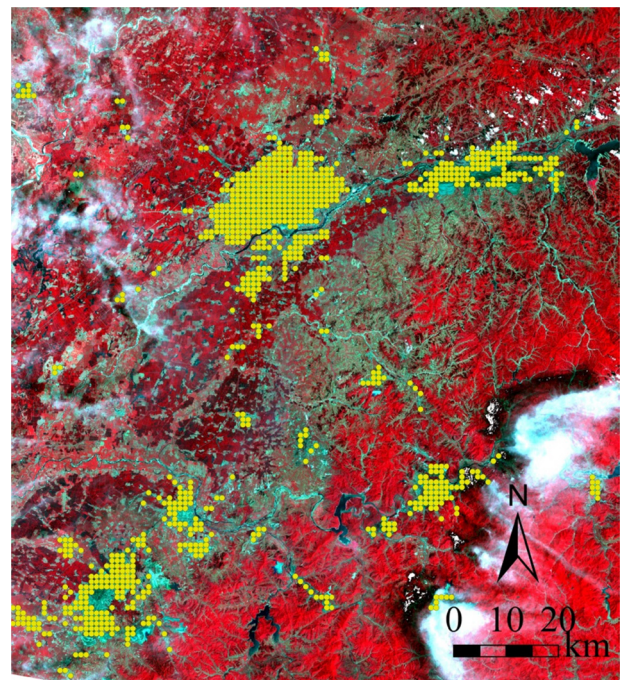

Fig. 3. Selection of desaturation PIFs: Points in yellow denote desaturated PIFs.

Table 1
Normalized thresholds determined using desaturation PIFs and linear regression method, 2000–2010.

DMSP datasets	Collected year	R square	α	β	Normalized threshold
F142000	2000	–	–	–	–
F152000	2000	0.90	6.87	0.92	43.87
F152001	2001	0.86	4.23	0.91	40.59
F152002	2002	0.89	3.87	0.98	43.03
F152003	2003	0.90	−1.28	0.99	38.34
F152004	2004	0.86	0.25	0.99	40.03
F162005	2005	0.83	3.77	0.95	41.61
F152006	2006	0.78	6.29	0.92	42.90
F162006	2006	0.80	6.21	0.96	44.51
F162007	2007	0.83	17.91	0.76	48.49
F162008	2008	0.66	11.48	0.92	48.31
F162009	2009	0.67	17.10	0.87	51.91
F182010	2010	0.55	24.97	0.75	54.94

values and urban areas determined with Landsat images as ground truth, we assessed the effectiveness and accuracy of our method.

Confusion matrix (also called error matrix) and overall accuracy (OA) measure have been used in previous studies for evaluating the spatial accuracy of urban areas extracted using DMSP-OLS data against Landsat TM/ETM+ data (30 m) (Henderson et al., 2003; Liu et al., 2012). However, as indicated by Kubat, Holte, and Matwin (1997), OA may not be an adequate measure in evaluating the accuracy of a classification when the dataset is imbalanced. According to Kubat, Holte, and Matwin (1998), a dataset is imbalanced if the classification categories are not approximately equally represented. Because the spatial extent of rural areas significantly outweighs that of urban areas in our study, we were essentially performing urban-rural classification based on an imbalanced DMSP-OLS dataset. Thus we adopted the geometric mean method proposed by Kubat et al. (1998) in assessing the spatial accuracy of this study's classification results. The geometric mean measure (g-mean) is computed with Eq. (4), using entries in the confusion matrix.

$$g\text{-mean} = \sqrt{\frac{d}{c+d} \times \frac{d}{b+d}} \qquad (4)$$

where d is the number of matched urban pixels, b and c are numbers of mismatched pixels in classification between DMSP-OLS-based result and Landsat-based result.

For each year and dataset, F152002, F152006, F162006, F162009 and F182010, g-mean was calculated. In addition, for the purpose of comparison with previous research, OA measure was also computed for each year and dataset. The results are summarized in Table 2.

As shown in Table 2, the threshold values estimated by desaturated PIF-based linear method and the optimal threshold values determined with Landsat TM images are very similar, with differences are less than 1.0. The urban areas detected with our estimated thresholds are mostly in line with those directly interpreted from Landsat imagery. The relative error of the estimated urban area is less than ±2% for all years except for 2010 (6.43%). For comparison, the OA and g-mean values were calculated for the four years of validation (Table 2). It can be seen that the OA values for our results are above 93% for all the four years. In contrast, this value is

79.7% for Beijing, 92.6% for San Francisco, and 99.10% for Lhasa in Henderson et al. (2003) research. Similarly, the OA value is 79.93% for Beijing, 83.82% for Chengdu, and 84.46% for Zhengzhou in Liu et al. (2012) study. The spatial accuracy of our results is even higher if evaluated by g-mean measure. The g-mean value is well above 67% for our result in each of the validation years. It is much higher than those calculated based on the confusion matrix provided in the studies of Henderson et al. (2003) and Liu et al. (2012). In Henderson et al. (2003), g-mean value is 4.86% for Lhasa, 49.12% for Beijing, and 65.02% for San Francisco. In Liu et al. (2012), this measure ranges from 31.62% for Beijing, 60.58% for Zhengzhou, to 61.68% for Chengdu. These comparisons indicate that urban detection results in this study are more accurate than those in the previous studies. All these assessment indices clearly demonstrate that our desaturated PIF-based linear regression method is effective and accurate.

Fig. 4 shows the scatter plots of the DN values of pixels within such desaturated PIFs between the reference year and each subsequent year of validation.

In our analysis, we assumed desaturated PIFs are temporally stable and invariant for eleven years between 2000 and 2010, and derived the threshold values for these years based on the reference year 2000. This assumption of the temporal stability and invariance of desaturated PIFs are in fact more valid within a relatively short-term period than for a long time span. To explore the impact of the time series' length, we also ran our normalization method and evaluated the results for two shorter periods by dividing the 2000–2010 time series into two sub time series: 2000–2005 and 2006–2010. Instead of using the year 2000, we used the year 2006 as the reference year for the second sub time series (2006–2010) and the optimal threshold value for 2006 was determined by using 2006 Landsat TM image and the iterative searching method.

The estimated urban detection thresholds and extracted urban areas for 2009 and 2010 by linear regression method with the reference year 2006 are more accurate than those obtained with 2000 as the reference year, especially for the year of 2010 (Table 3).

In addition to the apparent improvement in estimated thresholds and detected urban areas, the scatter plots (Fig. 5) and R^2 value also indicate that the linear relationship is more reliable and evident when year 2006, instead of year 2000, was used for the analysis of 2006–2010 sub-period.

Table 2
Validation of desaturation PIFs-based linear regression method with 2000 as the reference year.

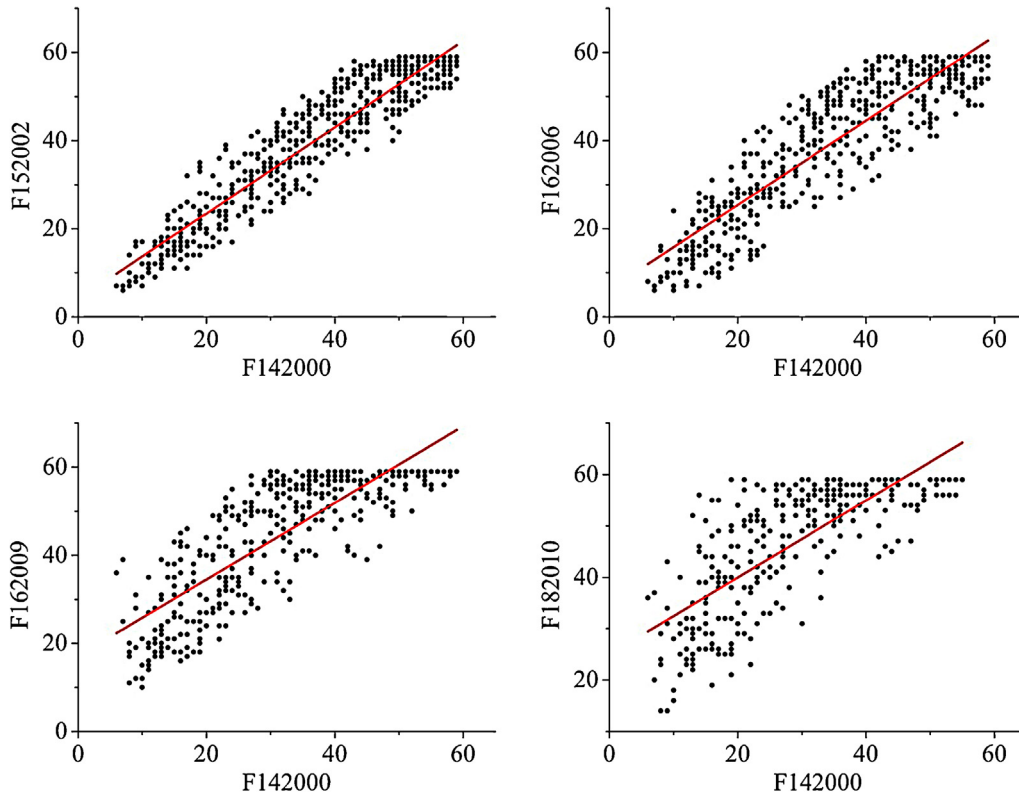| DMSP datasets	Optimal threshold	R square	α	β	Normalized threshold	Estimated area (km^2)	Actual area (km^2)	Relative error	Overall accuracy	g-Mean
F142000	40	–	–	–	–	969.38	955.31	1.47%	95.88%	67.10%
F152002	44	0.89	3.87	0.98	43.03	1002.00	1006.68	−0.46%	95.84%	68.52%
F152006	43	0.78	6.29	0.92	42.90	1134.68	1150.99	−1.42%	94.97%	67.99%
F162006	45	0.80	6.21	0.96	44.51	1172.10	1150.99	1.83%	94.88%	67.45%
F162009	52	0.67	17.10	0.87	51.91	1366.99	1390.71	−1.71%	94.58%	69.83%
F182010	56	0.55	24.97	0.75	54.94	1558.79	1464.55	6.43%	93.86%	68.82%

Fig. 4. Scatter plots of the DN values of the target years against the DN values of the reference year (2000) for pixels within desaturated PIFs. The solid line stands for the trend line of regression equation.

Table 3
Validation of desaturation PIFs-based linear regression method with 2006 as the reference year.

DMSP datasets	Optimal threshold	R square	α	β	Normalized threshold	Estimated area (km^2)	Actual area (km^2)	Relative error	Overall accuracy	g-Mean
F162006	45	–	–	–	44.51	1172.10	1150.99	1.83%	94.88%	67.45%
F162009	52	0.82	13.56	0.84	51.58	1366.99	1390.71	−1.71%	94.58%	69.83%
F182010	56	0.73	21.40	0.76	55.53	1486.96	1464.55	1.53%	93.93%	68.43%

4.4. Spatio-temporal evolution of Central Liaoning urban agglomeration

The urban areas of the Central Liaoning urban agglomeration were extracted from DMSP-OLS stable nighttime light data for the period of 2000–2010 based on the desaturated PIFs and the linear regression normalization approach. To ensure the robustness and reliability, TM imageries acquired in 2000 and 2006 were used as references to perform a two-stage normalization. Namely, the nighttime light images acquired during 2000–2010 were grouped into two sub periods: 2000–2005, 2006–2010. The reference years for the two sub periods are 2000 and 2006, respectively. Landsat TM images are available for these two years, based on which the optimal urban detection threshold values for these two reference years were determined. The urban detection threshold and corresponding urban areas for
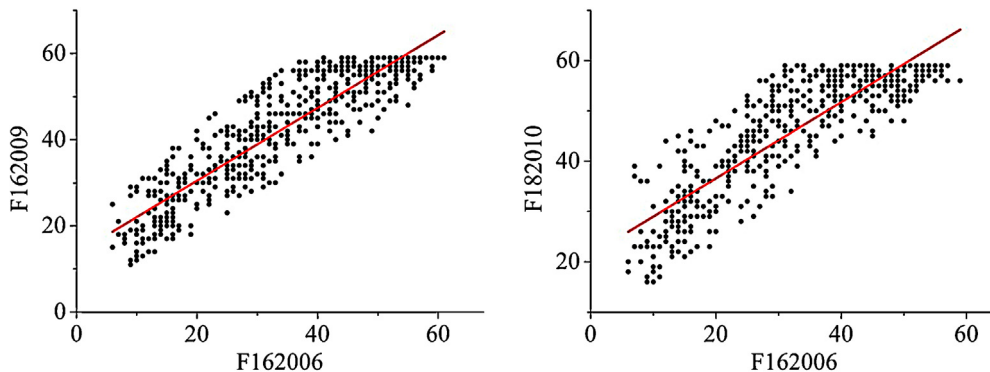

Fig. 5. Scatter plots of the DN values of the target years against the DN values of the reference year (2006) for pixels within desaturated PIFs. The solid line stands for the trend line of regression equation.
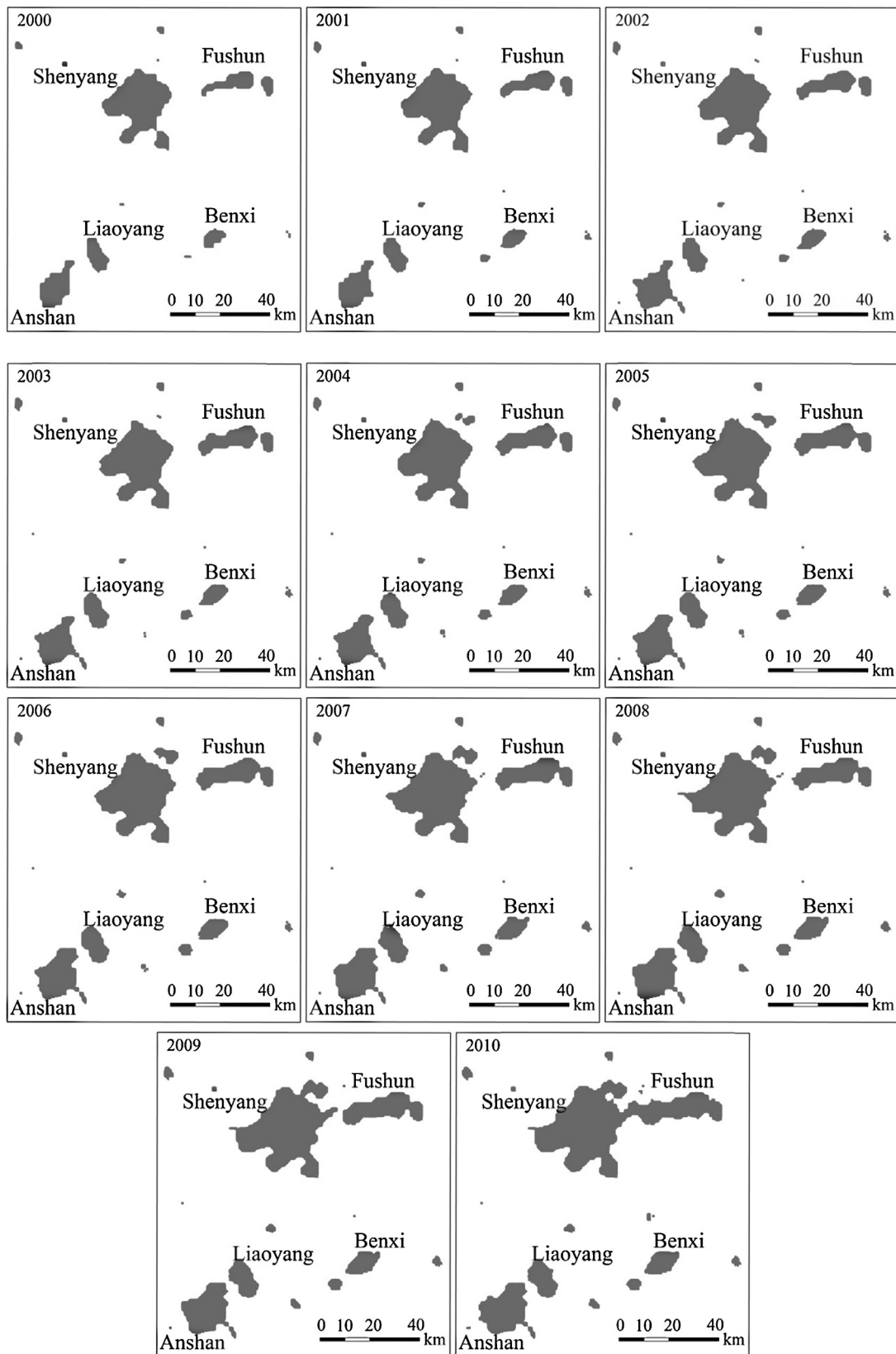
Fig. 6. Spatial and temporal dynamics of Central Liaoning urban agglomeration extracted from DMSP nighttime light data.

every year of these sub periods were determined using the linear regression method and mapped in ArcGIS. The time series urban area maps during the 2000–2010 period are displayed in Fig. 6.

As shown in Fig. 6, during the 2000–2010 period, the urban area of the Central Liaoning region increased very fast. Results show that the total urban area of this region increased by 54.09% from 965 km^2 to 1487 km^2. And in the first stage (2000–2005), the Central
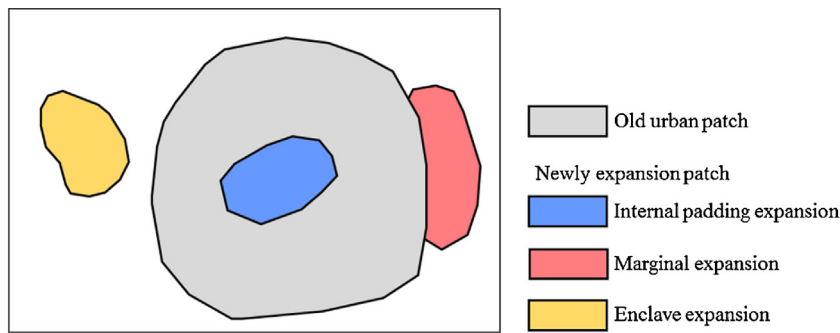
Fig. 7. Schematic diagram for different types of urban expansion.

Liaoning urban agglomeration experienced a relatively steady growth at an annual urban expansion rate of 3.16%. In the second stage (2006–2010), the urban expansion was accelerated to an annual rate of 6.92%, which is over twice as fast as that in the first stage.

For better understanding of the spatio-temporal evolution of the Central Liaoning urban agglomeration, a landscape expansion index (LEI) method proposed by Wu, Gong, Li, and Zhou (2012) was employed. In contrast with the traditional landscape indices, the landscape expansion index can capture more dynamic information on the evolution process of landscape patterns. LEI is defined by Eq. (5) (Wu et al., 2012).

$$LEI = \frac{A_p - A_0}{A_p + A_0} \qquad (5)$$

where LEI is the landscape expansion index, A_p stands for the area of newly expanding urban patch and A_0 refers to the area of old urban patch which is adjacent to the newly expanding patch.

Wu et al. (2012) believed that expansion patterns could be identified by using the LEI method, namely the adjacent expansion pattern and the external expansion pattern. As shown in Fig. 7, the internal padding expansion and marginal expansion belong to the adjacent expansion pattern, because both of them start from the boundary of an existing urban patch. And enclave expansion belongs to the external expansion pattern due to its disconnection with the existing urban patches. In term of the spatial effect, the adjacent expansion pattern is reflected by the increase in the area of urban patches, while the external expansion pattern raises the number of urban patches. Normally, the LEI values are within the interval of (−1, 1]. When A_0 equals 0, and LEI equals 1, there is no old urban patch adjacent to the newly expanding urban patch. In this case, the expansion pattern is manifested by the external expansion pattern. When LEI is within the interval of (−1, 1), the spatial expansion follows the adjacent expansion pattern.

Besides the LEI, MLEI was also introduced by Wu et al. (2012). MLEI is calculated by Eq. (6).

$$MLEI = \sum_{i=1}^{n} \frac{LEI_i}{n} \qquad (6)$$

where MLEI is the mean value of LEIs of all the newly expanded urban patches, LEI_i is the LEI value of new urban patch i, and n is the total number of new urban patches. Normally, a larger MLEI indicates that there are more new urban patches following the external expansion pattern, and thus the urban expansion of the region is in a diffusion phase. Conversely, a smaller MLEI implies that there are more new urban patches developing by the adjacent expansion pattern, and the urban expansion of the region tends to be more compact in spatial form.

For each of the two periods, 2000–2005 and 2006–2010, the extracted urban areas in the beginning year from DMSP-OLS data were considered old urban patches, and the expanded urban areas in the ending year were regarded as new urban expansion patches. The LEI value of each urban expansion patch was calculated. Based on the value of LEI, these expanding urban patches were categorized as belonging to either the adjacent expansion pattern or the external expansion pattern (see Fig. 8). The number of patches and the increase in geographic area of each category were summarized in Table 4. In addition, MLEI values of newly expanding urban patches for the period of 2000–2005 and 2006–2010 were also calculated and reported in Table 4.

Dietzel, Herold, Hemphill, and Clarke (2005) believed that the urban expansion process is manifested by temporal oscillation between the phases of diffusion and coalescence based on the urban growth phases theory (Cressy, 1939; Duncan, Sabagh, & Van Arsdol, 1962; Winsborough, 1962). In the initial stage, new urban growth point (towns) emerged in the urban periphery, and the number of urban patches increased. This could be considered a diffusion process. Later, with the expansion of urban patches, the distances between them decreased and urban patches gradually merged together, suggesting a stage of coalescence. As shown in Fig. 8 and Table 4, during the 2000–2005 period only 6 patches were in the external expansion pattern, accounting for 25% of the total number of expanding urban patches and 4% of total expanding area. During the 2006–2010 period, merely 3 patches belonged to the external expansion pattern, constituting just 6% of the total number of expanding urban patches and 2% of the total expanding area. These results, along with the negative values of MLEI, clearly suggest that the adjacent expansion was the leading spatial pattern for the development of the Central Liaoning urban agglomeration in the period between 2000 and 2010. Meanwhile, the characteristics of a coalescence phase of this urban expansion process are similarly evident. A further and closer examination of the Central Liaoning urban agglomeration's adjacent urban

Table 4
Measures of spatial expansion patterns of Central Liaoning urban agglomeration, 2000–2005 and 2006–2010.

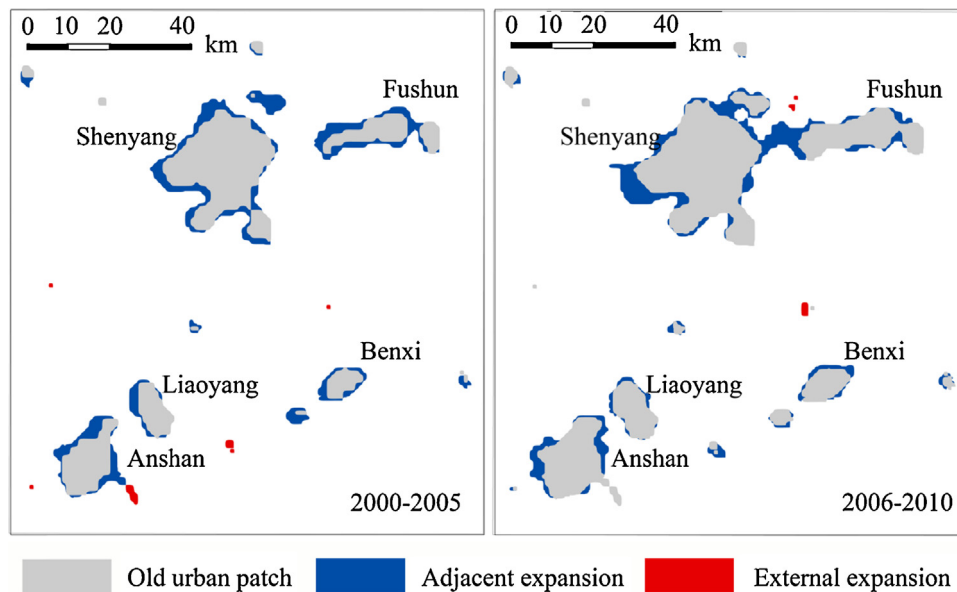| Period	Number of patches in adjacent expansion pattern	Number of patches in external expansion pattern	Total number of patches	Increased area in adjacent expansion pattern (km²)	Increased area in external expansion pattern (km²)	Total increased area (km²)	MLEI
2000–2005	24	6	30	408.83	16.57	425.4	−0.17
2006–2010	47	3	50	385.13	8.49	393.62	−0.72

Fig. 8. Urban expansion patterns of Central Liaoning agglomeration, 2000–2005 and 2006–2010.

expansion also reveals that it mainly followed linear (Camagni, Gibelli, & Rigamonti, 2002) and amalgamated forms (Zeng, Sui, & Li, 2005a,b). For example, Shenyang stretched in several directions along the transportation corridors, and some isolated urban patches were gradually merged into the major urban built-up area. Obviously, the linear expansion would lead to decentralization, while amalgamated expansion tended to promote further enlargement of the urban agglomeration. The two forms of spatial expansion largely coincided with industrial relocations, as well as the construction of new economic development zones and industrial districts in the region. These findings largely echo those from the studies of the Pearl River delta, Yangtze River delta and Bohai Rim in China for the same period of time (Fan, Ma, Zhou, & Zhou, 2013; Liu et al., 2009; Wang, Wang, Li, & Dong, 2012).

Actually, spatial coalescence did not just happen between each city and its surrounding areas. The coalescence of neighboring metropolitan areas in the Central Liaoning urban agglomeration is also apparent. The expanding metropolitan areas within the urban agglomeration were approaching and coalescing with each other over time. For example, the distance between urban areas of Shenyang and Fushun was 11.91 km in 2000, and the two conjoined in 2010. The spatial expansion of Anshan and Liaoyang metropolitan areas led to the decrease in the distance between the two metropolitan areas from 5.45 km in 2000 to 3.08 km in 2010.

The Central Liaoning urban agglomeration is expanding rapidly primarily through the enlargement of existing cities in the system, rather than the new development of small towns. This large-scale urban development is directly related to the economic growth and restructuring, as well as the construction of infrastructure (e.g. highway network) in Liaoning Province. The old manufacturing heartland of Liaoning, centered at Shenyang, is restructuring toward a more diversified economy based on economic specialization and increasing interaction among cities and between cities and hinterlands. This economic momentum has propelled and will continue to drive the expansion and shape the spatial organization of the Central Liaoning urban agglomeration.

5. Discussions

The concept and method of pseudo invariant areas and stable pixels in time series images have been used in many remote sensing studies (Coppin & Bauer, 1994; Hall et al., 1991; Lenney et al., 1996).

The focus of our paper is to develop a new, PIF-based technique to normalize time series DMSP-OLS nighttime light image, and more importantly, determine the urban detection threshold values for all years, using ancillary reference data only for the base year of the time series.

Urbanization is usually an irreversible process. Once a rural area is converted into urban area, it would remain urban and it's nearly impossible for the area to be converted back to rural. The overall nighttime light intensity of many urban districts, such as densely populated residential neighborhoods, would remain stable and invariant over time once they were established. Such urban districts can be used as PIFs to normalize multi-temporal DMSP-OLS light images. In this study, we use desaturated PIFs in different years of DMSP-OLS images to capture the type of transformation relationship to help normalize time series data and determine different urban detection threshold values.

When conducting urban area extraction using determined threshold values, we implemented a safeguard or control such that urban pixels extracted in the previous year nighttime light image would remain urban in subsequent years. The derived threshold value in each year is practically more important in facilitating the search for newly urbanized areas. In this way, we ensured that urban areas detected would be consistent in the time series and follow a spatial pattern of continuous outward growth as reflected by the concentric zone model.

Although the concept of and method based on PIFs proved work well in empirical analysis, we recognized that the length of the time series could somewhat affect the analytical results. We evaluated this effect by dividing the 2000–2010 time series into two sub time series with different reference years, and demonstrated the improvement in the accuracy of the estimated threshold values and the detected urban areas, for shorter time series. From a more practical perspective, the assumption of temporal stability and invariance for PIFs is more valid for a shorter period of time.

The DMSP-OLS stable nighttime light images often suffer from the saturation problems. Such problem occurred in the urban centers and intensive industrial districts, particularly in developed countries. Our experiments suggest that not only fully saturated pixels but also nearly saturated pixels could distort the analysis results of our robust linear regression method. Thus, when creating desaturated PIFs, nearly saturated pixels were also removed to avoid the calibration of biased regression equations. In future

applications, we will further examine the effects of nearly saturated pixels on the implementation of our techniques. In addition, the use of reliance calibrated nighttime light images from sensors with low-gain setting is expected to improve the threshold accuracy of our robust linear regression method since the pixel saturation problem is reduced or avoided in these low-gain nighttime light images.

It is obvious that a key issue in applying our proposed method is the correct determination of the PIFs. In some rapidly developed cities, established urban districts have experienced substantial revitalization over time, resulting in the change in land use structure and land use densities. The redevelopment of these existing and established urban districts, as well as the evolution of newly developed urban edges may lead to the intensification of night lights, thus making the identification of desaturated PIFs more challenging. More thorough understanding of the structure and development of the city in question is very important in facilitating the delineation of PIFs when applying this method.

6. Conclusions

A long-term time series of stable DMSP-OLS nighttime light data have been collected globally. However, the nighttime light images are not directly comparable across multiple years, due to the variation in atmospheric conditions from year to year and the periodic change in satellite sensor and sensor gain settings. This problem has hindered the use of time series nighttime light data for long-term urban growth analysis. Although many efforts have been made to normalize multi-temporal DMSP-OLS images, improving image data continuity and comparability and effectively extracting dynamic urban changes remain a great challenge. In this paper, we, for the first time, systematically introduced the concept of Pseudo Invariant Features (PIFs) and presented a novel numerical method, based on PIFs, for normalizing multi-temporal DMSP nighttime light images and extracting time series urban area maps. Our methods enable rapid extraction of urban areas and analysis of long-term urban dynamics using time series DMSP-OLS nighttime light images with only limited high resolution ancillary data.

Our methods were successfully applied to the study of Central Liaoning region in China for the period between 2000 and 2010. The validity and accuracy of urban detection threshold values and corresponding urban areas estimated were evaluated against the reference urban areas visually interpreted from Landsat TM images. Our evaluations indicated that the robust linear regression method based on desaturated PIFs was effective and accurate. In almost every year of the time series, the error in the estimation of urban detection threshold values was less than 1.0, and the relative error of the detected urban areas was smaller than 2%. The spatial accuracy (g-mean) was above 67%, which is better than previous studies. Using landscape indices along with extracted urban areas, our results also depicted and highlighted the spatial pattern in the growth of Central Liaoning urban agglomeration which was obviously led and dominated by the adjacent expansion. Furthermore, it was clear that the spatial development of this urban agglomeration has entered the coalescence phase during the first decade of the 21st century. Individual metropolitan areas have become increasingly interrelated and integrated in this mega urban space. These results clearly demonstrated the applicability of our techniques in urban growth analysis and urban growth planning. By applying our techniques to the time series DMSP-OLS nighttime light images from 2000 to 2010, we demonstrated that the long-term DMSP nighttime image time series is a useful data source for studying the spatio-temporal evolution of urban systems at regional scale.

Compared with government statistics and census, time series DMSP-OLS nighttime light data are more objective, and reflect the natural distribution and evolution of economic activities in a study area, thus have enormous potential to shed light on urbanization processes at different spatial scales. We believe that our new methods are promising and will undoubtedly further more sophisticated and accurate research on the spatial and temporal change in urbanization dynamics at national, continental, and global scales with the time series DMSP-OLS nighttime light image data. We plan to apply the methods to the study of China's urban dynamics at the national scale.

References

Burgess, E. W. (1925). The growth of the city. In R. E. Park, R. E. Park, et al. (Eds.), *The city*. Chicago: Chicago University Press.

Camagni, R., Gibelli, M. C., & Rigamonti, P. (2002). Urban mobility and urban form: The social and environmental costs of different patterns of urban expansion. *Ecological Economics*, 40(2), 199–216. http://dx.doi.org/10.1016/S0921-8009(01)00254-3

Canty, M. J., & Nielsen, A. A. (2008). Automatic radiometric normalization of multitemporal satellite imagery with the iteratively re-weighted MAD transformation. *Remote Sensing of Environment*, 112(3), 1025–1036. http://dx.doi.org/10.1016/j.rse.2007.07.013

Clark, B., Suomalainen, J., & Pellikka, P. (2011). The selection of appropriate spectrally bright pseudo-invariant ground targets for use in empirical line calibration of SPOT satellite imagery. *ISPRS Journal of Photogrammetry and Remote Sensing*, 66(4), 429–445. http://dx.doi.org/10.1016/j.isprsjprs.2011.02.003

Coppin, P. R., & Bauer, M. E. (1994). Processing of multitemporal Landsat TM imagery to optimize extraction of forest cover change features. *IEEE Transactions on Geoscience and Remote Sensing*, 32(4), 918–927. http://dx.doi.org/10.1109/36.298020

Cressy, P. F. (1939). Population succession in Chicago, 1898–1930. *American Journal of Sociology*, 44(1), 59–69.

Croft, T. A. (1978). Night-time images of the Earth from space. *Scientific American*, 239, 68–79.

Dietzel, C., Herold, M., Hemphill, J. J., & Clarke, K. C. (2005). Spatio-temporal dynamics in California's Central Valley: Empirical links to urban theory. *International Journal of Geographical Information Science*, 19(2), 175–195. http://dx.doi.org/10.1080/13658810410001713407

Doll, C. N. H. (2008). *CIESIN thematic guide to night-time light remote sensing and its applications*. Palisades, NY: Center for International Earth Science Information Network of Columbia University. Retrieved from http://sedac.ciesin.columbia.edu/tg/

Duncan, B., Sabagh, G., & Van Arsdol, M. D. (1962). Patterns of city growth. *American Journal of Sociology*, 67(4), 418–429.

Elvidge, C. D., Baugh, K. E., Kihn, E. A., Kroehl, H. W., & Davis, E. R. (1997). Mapping city lights with nighttime data from the DMSP Operational Linescan System. *Photogrammetric Engineering and Remote Sensing*, 63(6), 727–734.

Elvidge, C. D., Baugh, K. E., Kihn, E. A., Kroehl, H. W., Davis, E. R., & Davis, C. W. (1997). Relation between satellite observed visible-near infrared emissions, population, economic activity and electric power consumption. *International Journal of Remote Sensing*, 18(6), 1373–1379.

Elvidge, C. D., Baugh, K. E., Dietz, J. B., Bland, T., Sutton, P. C., & Kroehl, H. W. (1999). Radiance calibration of DMSP-OLS low-light imaging data of human settlements. *Remote Sensing of Environment*, 68(1), 77–88. http://dx.doi.org/10.1016/s0034-4257(98)00098-4

Elvidge, C. D., Jeffrey, S., Ingrid, N., Benjamin, T., Vinita Ruth, H., Kimberly, B., et al. (2004). Area and positional accuracy of DMSP night lights data. In *Remote sensing and GIS accuracy assessment* (pp. 281–292). CRC Press. http://dx.doi.org/10.1201/9780203497586.ch20

Elvidge, C. D., Erwin, E. H., Baugh, K. E., Ziskin, D., Tuttle, B. T., Ghosh, T., et al. (2009). Overview of DMSP night-time lights and future possibilities. In *Urban remote sensing event, 2009 Joint* (pp. 1–5). http://dx.doi.org/10.1109/URS.2009.5137749

Elvidge, C. D., Ziskin, D., Baugh, K. E., Tuttle, B. T., Ghosh, T., Pack, D. W., et al. (2009). A fifteen year record of global natural gas flaring derived from satellite data. *Energies*, 2(3), 595–622. http://dx.doi.org/10.3390/en20300595

Fan, J., Ma, T., Zhou, C., & Zhou, Y. (2013). Changes in spatial patterns of urban landscape in Bohai Rim from 1992 to 2010 using DMSP-OLS data. *Journal of Geo-Information Science*, 15(2), 280–288 [In Chinese].

Hadjimitsis, D. G., Clayton, C. R. I., & Retalis, A. (2009). The use of selected pseudo-invariant targets for the application of atmospheric correction in multi-temporal studies using satellite remotely sensed imagery. *International Journal of Applied Earth Observation and Geoinformation*, 11(3), 192–200. http://dx.doi.org/10.1016/j.jag.2009.01.005

Hall, F. G., Strebel, D. E., Nickeson, J. E., & Goetz, S. J. (1991). Radiometric rectification: Toward a common radiometric response among multi-date, multisensor images. *Remote Sensing of Environment*, 35(1), 11–27. http://dx.doi.org/10.1016/0034-4257(91)90062-B

Harris, C. D., & Ullman, E. L. (1945). The nature of cities. *Annals of the American Academy of Political and Social Science*, 242(1), 7–17.

He, C., Shi, P., Li, J., Chen, J., Pan, Y., Li, J., et al. (2006). Restoring urbanization process in China in the 1990s by using non-radiance calibrated DMSP/OLS nighttime

light imagery and statistical data. *Chinese Science Bulletin, 51*(7), 856–861. http://dx.doi.org/10.1007/s11434-006-2006-3

Henderson, M., Yeh, E. T., Gong, P., Elvidge, C., & Baugh, K. (2003). Validation of urban boundaries derived from global night-time satellite imagery. *International Journal of Remote Sensing, 24*(3), 595–609. http://dx.doi.org/10.1080/01431160304982

Hoyt, H. (1939). *The structure and growth of residential neighbourhoods in American cities.* Washington, DC: Government Printing Office.

Imhoff, M. L., Lawrence, W. T., Stutzer, D. C., & Elvidge, C. D. (1997). A technique for using composite DMSP/OLS 'city lights' satellite data to map urban area. *Remote Sensing of Environment, 61*(3), 361–370. http://dx.doi.org/10.1016/s0034-4257(97)00046-1

Kubat, M., Holte, R., & Matwin, S. (1997). Learning when negative examples abound. In *Proceedings of the 14th international conference on machine learning, 1224* (pp. 179–186). San Francisco: Morgan Kaufmann. http://dx.doi.org/10.1007/3-540-62858-4_79

Kubat, M., Holte, R., & Matwin, S. (1998). Machine learning for the detection of oil spills in satellite radar images. *Machine Learning, 30*, 195–215. http://dx.doi.org/10.1023/A:1007452223027

Lenney, M. P., Woodcock, C. E., Collins, J. B., & Hamdi, H. (1996). The status of agricultural lands in Egypt: The use of multitemporal NDVI features derived from landsat TM. *Remote Sensing of Environment, 56*(1), 8–20. http://dx.doi.org/10.1016/0034-4257(95)00152-2

Liu, J., Zhan, J., & Deng, X. (2005). Spatio-temporal patterns and driving forces of urban land expansion in China during the economic reform era. *AMBIO: A Journal of the Human Environment, 34*(6), 450–455. http://dx.doi.org/10.1579/0044-7447-34.6.450

Liu, X., Li, X., Chen, Y., Qin, Y., Li, S., & Chen, M. (2009). Landscape expansion index and its applications to quantitative analysis of urban expansion. *Acta Geographica Sinica, 64*(12), 1430–1438 [In Chinese].

Liu, Z., He, C., Zhang, Q., Huang, Q., & Yang, Y. (2012). Extracting the dynamics of urban expansion in China using DMSP-OLS nighttime light data from 1992 to 2008. *Landscape and Urban Planning, 106*(1), 62–72. http://dx.doi.org/10.1016/j.landurbplan.2012.02.013

Mann, P. (1965). *An approach to urban sociology.* London: Routledge.

Milesi, C., Elvidge, C. D., Nemani, R. R., & Running, S. W. (2002). Impact of urban sprawl on net primary productivity in the Southeastern United States. In *IEEE international on geoscience and remote sensing symposium, 2002. IGARSS '02* (pp. 2971–2973).

Murdie, R. A. (1969). *Factorial ecology of metropolitan Toronto, 1951–1961. Research paper No. 116.* Department of Geography, University of Chicago.

NGDC. (2011). *Global DMSP-OLS nighttime lights time series (version 4).* Retrieved from http://www.ngdc.noaa.gov/dmsp/downloadV4composites.html

Philpot, W., & Ansty, T. (2011). Analytical description of pseudo-invariant features (PIFs). In *6th international workshop on the analysis of multi-temporal remote sensing images* Trento, (pp. 53–56).

Schott, J. R., Salvaggio, C., & Volchok, W. J. (1988). Radiometric scene normalization using pseudoinvariant features. *Remote Sensing of Environment, 26*(1), 1–16. http://dx.doi.org/10.1016/0034-4257(88)90116-2

Seto, K. C., & Fragkias, M. (2005). Quantifying spatiotemporal patterns of urban land-use change in four cities of China with time series landscape metrics. *Landscape Ecology, 20*(7), 871–888. http://dx.doi.org/10.1007/s10980-005-5238-8

Shevsky, E., & Bell, W. (1955). *Social area analysis: Theory, illustrative application and computational procedures.* Stanford, CA: Stanford University Press.

Small, C., Pozzi, F., & Elvidge, C. D. (2005). Spatial analysis of global urban extent from DMSP-OLS night lights. *Remote Sensing of Environment, 96*(3–4), 277–291. http://dx.doi.org/10.1016/j.rse.2005.02.002

Small, C., Elvidge, C. D., Balk, D., & Montgomery, M. (2011). Spatial scaling of stable night lights. *Remote Sensing of Environment, 115*(2), 269–280. http://dx.doi.org/10.1016/j.rse.2010.08.021

Sutton, P. C. (2003). A scale-adjusted measure of "Urban sprawl" using nighttime satellite imagery. *Remote Sensing of Environment, 86*(3), 353–369. http://dx.doi.org/10.1016/s0034-4257(03)00078-6

Sutton, P., Roberts, D., Elvidge, C., & Baugh, K. (2001). Census from heaven: An estimate of the global human population using night-time satellite imagery. *International Journal of Remote Sensing, 22*(16), 3061–3076. http://dx.doi.org/10.1080/01431160010007015

Sutton, P. C., Cova, T. J., & Elvidge, C. D. (2006). Mapping "Exurbia" in the conterminous United States using nighttime satellite imagery. *Geocarto International, 21*(2), 39–45. http://dx.doi.org/10.1080/10106040608542382

Theobald, D. M. (2001). Land-use dynamics beyond the American urban fringe. *Geographical Review, 91*(3), 544–564. http://dx.doi.org/10.1111/j.1931-0846.2001.tb00240.x

Wang, C. P., Wang, H. W., Li, C. M., & Dong, R. C. (2012). Analysis of the spatial expansion characteristics of major urban agglomerations in China using DMSP/OLS images. *Acta Ecologica Sinica, 32*(3), 942–954 [In Chinese].

Winsborough, H. H. (1962). City growth and city structure. *Journal of Regional Science, 4*(2), 35–50.

Witmer, F. D. W., & O'Loughlin, J. (2011). Detecting the effects of wars in the Caucasus regions of Russia and Georgia using radiometrically normalized DMSP-OLS nighttime lights imagery. *GIscience and Remote Sensing, 48*(4), 478–500. http://dx.doi.org/10.2747/1548-1603.48.4.478

Wu, P., Gong, H., Li, X., & Zhou, D. (2012). Analysis of agricultural cultivation based on a new landscape expansion index: A case study in Guishui river basin, China. *Journal of Agricultural Science, 4*(4), 151–162. http://dx.doi.org/10.5539/jas.v4n4p151

Zeng, H., Sui, D. Z., & Li, S. J. (2005). Linking urban field theory with GIS and remote sensing to detect signatures of rapid urbanization on the landscape: Toward a new approach for characterizing urban sprawl. *Urban Geography, 26*(5), 410–434. http://dx.doi.org/10.2747/0272-3638.26.5.410

Zeng, H., Sui, D. Z., & Li, S. (2005). Linking urban field theory with GIS and remote sensing to detect signatures of rapid urbanization on the landscape: Toward a new approach for characterizing urban sprawl. *Urban Geography, 26*(5), 410–434.

Zhang, P. (2008). Revitalizing old industrial base of Northeast China: Process, policy and challenge. *Chinese Geographical Science, 18*(2), 109–118. http://dx.doi.org/10.1007/s11769-008-0109-2

Zhang, Q., & Seto, K. C. (2011). Mapping urban dynamics at regional and global scales using multi-temporal DMSP/OLS nighttime light data. *Remote Sensing of Environment, 115*(9), 2320–2329. http://dx.doi.org/10.1016/j.rse.2011.04.032

Zhang, L., Wu, J., Zhen, Y., & Shu, J. (2004). A GIS-based gradient analysis of urban landscape pattern of Shanghai metropolitan area, China. *Landscape and Urban Planning, 69*(1), 1–16. http://dx.doi.org/10.1016/j.landurbplan.2003.08.006